Application of the Ultrasound Doppler Velocimetry in a Czochralski crystal growth model experiment

Andreas Cramer, Josef Pal and Gunter Gerbeth
Institute of Safety Research, Magneto-Hydrodynamics Division
Forschungszentrum Dresden-Rossendorf, P.O. Box 51 01 19, 01314 Dresden, Germany

The present work is concerned with ultrasound and temperature measurements in a Czochralski crystal growth model experiment. In the Czochralski growth, primary strong horizontal temperature gradients are present at the solidification front, which should lead to an axisymmetric flow pattern in the melt volume. To study the flow structure a modified Rayleigh-Bénard configuration was built up in which the upper thermal boundary condition in a Czochralski system is accounted for by a partially cooled surface. The measurements show, that rather a large scale flow pattern develops known as wind in real Rayleigh–Bénard configurations. The wind was always found as the only stable flow pattern for all performed Grashof numbers. Applying a rotating magnetic field (RMF) to the melt volume, the wind starts to co-rotate with the RMF. By analogue with the superposition of the primary and the secondary flow in an RMF, the swirl evoked by the RMF is also superimposed to the wind without any remarkable interaction. Not until the weaker secondary flow produced by the RMF becomes similar in vigour to the buoyant wind does the flow structure in the modified Rayleigh-Bénard system change basically. The results show the applicability of the Ultrasound Doppler Velocimetry (UDV) in the detection and identification of complex flow patterns.

Keywords: Ultrasound Doppler Velocimetry, Temperature gradients, Czochralski crystal growth, Fluid flow,

1 INTRODUCTION

Electromagnetic processing of materials provides the means to gain control of the flow in metallurgical and crystal growth tasks. Still to date, the strategy in quite a lot of work done on the field is to apply magnetic fields, observe their influence on the flow field, and to analyse the modification of the final product. A more promising approach goes the opposite direction: as flow control is merely a tool, the goal is to be expressed with objective functions. These targets are most reasonably formulated in terms of the relevant quantities, which are often distribution and transport of the scalars temperature and concentration. One example in Czochralski crystal growth is the ratio $r^* = \Delta T_h / \Delta T_v$ of the horizontal and the vertical temperature gradient within the silicon melt at the perimeter of the growing crystal.

Once an objective function is defined, the task formulation is to solve a multi-step inverse problem: a flow field that fulfils the target function is to be sought. Given this flow field, it has to be realised by means of applying magnetic fields, or, as is the case in crystal growth, the buoyant convection intrinsic to the process is to be accordingly controlled electromagnetically. Finally, a coil system producing the fields determined in the previous step has to be designed. As the problem is extraordinarily difficult if ever solvable, known results from the corresponding forward strategies are to be adopted for each step.

Prior describing the apparatus employed to study the effect of the RMF used hitherto on the ratio r^* and the flow field, the action of this field type on a cylindrical liquid metal volume is briefly recalled. An AC magnetic field of strength $\boldsymbol{B}_0$ applied to an electrical conductor induces an eddy current $\boldsymbol{j}$ within that medium. The interaction of $\boldsymbol{j}$ with the field that produced it results in a Lorentz force $\boldsymbol{F}_L = \boldsymbol{j} \times \boldsymbol{B}_0$, which may drive a flow in the case that the electrical conductor is liquid. In [1], $\boldsymbol{F}_L$ is expressed as

$$\boldsymbol{F}_L = \mathrm{Ta}\, r f(r,z)\boldsymbol{e}_\varphi, \mathrm{Ta} = \frac{\sigma \omega B_0^2 R^4}{2\rho\nu^2}, \qquad (1)$$

where the Taylor number Ta is a measure for the relative strength of the driving force, σ, ρ, and ν are electrical conductivity, density and kinematical viscosity of the melt, R is the radius of the liquid metal column, and ω is the frequency of the RMF. The shape function f vanishes at the top and the bottom walls. Eq. 1 is valid for the low-frequency and low-induction approximation. Low frequency means $\mu\sigma\omega R^2 < 1$ with μ being the magnetic permeability, whereas low-induction stands for the case that the characteristic angular velocity of the resulting flow is much smaller than the field frequency ω. The flow developing under the influence of an RMF is a primary swirl following the mere azimuthal direction of $\boldsymbol{F}_L$ in Eq. 1. Initiated by an imbalance between pressure and centrifugal force at non-vertical rigid walls, a meridional motion is superimposed. This secondary flow exhibits a toroidal structure with two vortices lying on top of each other, leading to a jet moving radially outward at mid-height of the liquid column [2].

2 EXPERIMENTAL SETUP

The apparatus, shown in Fig. 1, is a modified Rayleigh-Bénard configuration, in which the upper thermal boundary condition in a Czochralski system is accounted for by a partially cooled surface. This partial cooling covering approximately the same area as the growing crystal in an industrial facility is realised with a circular heat exchanger mounted concentrically within the upper lid. Some compromise had to be made with respect to the entity of all boundary conditions. The surface between the crystal and the crucible is free, whereas it is covered by a PTFE lid in the model. This construction was motivated by the thermal boundary condition. Both the heat exchanger at the top and the bottom heating plate are made from copper to approximate isothermal boundary conditions. This approach is further supported by a branched structure of flow channels machined into the copper parts. A precise control of temperatures is realised by supplying the heat exchanger and the bottom heater with coolant/heating fluid at high flow rate from thermostats having a large reservoir, the latter being regulated by a PID circuit. Differences to the set-point and inhomogeneity were monitored by platinum resistance wires mounted within the heat exchanger and the bottom heater at various positions and found to be less than 0.05 K. Water may be used as a coolant, whereas the aim to reach high temperature gradients necessitates a heating fluid with a high boiling point. The experiments were thus performed with silicone oil. It is noted that all copper parts in contact with the fluid are covered by a thin electrically insulating layer of aluminium oxide. Otherwise electric current may circulate between the fluid under investigation and those parts, which is likely to modify the distribution of the Lorentz force and in turn the flow structure.

A borosilicate glass pipe 90 mm in inner diameter and also in height was chosen for the reasons of being electrically insulating, relatively poor heat conducting so as to approach what is commonly referred to as adiabatic boundary condition, allowing transmission of ultrasound for flow measurements, and standing relatively high temperatures. Sealing of the cell is realised by clamping the glass cylinder between the bottom heater and the PTFE top cover by means of thread rods screwed into the bottom plate. Different thermal expansion coefficients of the constructional materials are accounted for with springs inserted between the PTFE disc and the upper fastening nuts. The upper limit on temperature is imposed by the o-rings, which are located in the annular grooves machined into the PTFE disc (c.f. Fig. 1) and the bottom heater. These sealings are made from highly fluorinated synthetic elastomer and may be used at permanent load up to 280 °C. During the measurements, the whole apparatus was embedded in mineral wool serving the minimisation of the lateral heat loss.

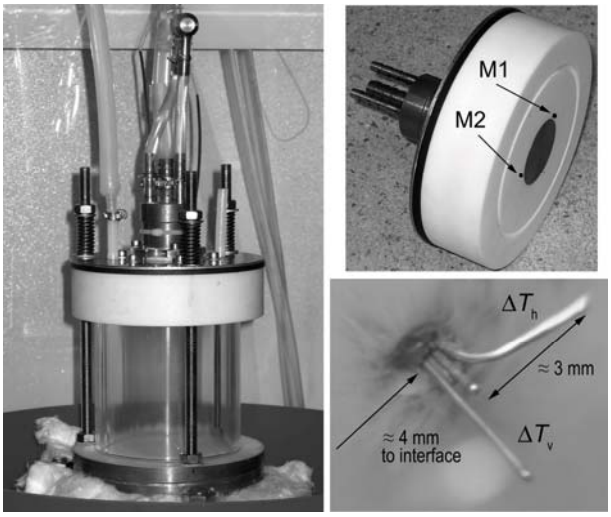

Figure 1: On the left a photo of the whole experimental setup, the right upper picture an oblique view from below of the PTFE top cover. M1 and M2 are the locations of the thermocouple-tripods close to the circumference of the heat exchanger. The right lower figure shows the equilateral-triangular arrangement of the three thermo-couples comprising a measuring point.

Temperatures in the melt are measured with mineral insulated type K thermocouples with protective tubes of 250 μm in total diameter. Three thermocouples in a triangular arrangement as shown in Fig. 1 allow determination of both horizontal and vertical temperature gradients. It can be seen, that two such tripods are mounted at the perimeter of the top heat exchanger. As we shall see immediately below, the advantage thereof is not restricted to having solely a second measuring station. Because of the relatively small size of the thermocouples, transients of temperature may be recorded together with the mean values. Ultrasound Doppler Velocimetry in conjunction with the presence of two metering points for the temperature gradients proves a valuable tool in the detection and the characterisation of non-axisymmtric convective patterns. Acoustic properties of the borosilicate glass and the smooth surface of the pipe permit attaching a transducer to the outside of that wall to measure the radial velocity component along the entire ultrasonic beam. UDV has matured during the past years and is commercially available from a variety of manufacturers to date. Here, a DOP2000 (Model 2032, Signal-Processing, Lausanne, Switzerland) was used. The principle of operation of UDV is described in the pioneering work of Takeda [3], and a demonstration of the ability to work for liquid metals may be found in [4].

The RMF was generated by the home-made MULTIpurpose MAGnetic field system, which is described in detail in [5]. Besides an RMF, MULTIMAG offers also other magnetic field types, even linear superpositions thereof. Such flexibility will certainly be the experimental basis for future work on the present topic of tailored flow control.

3 RESULTS

Naturally, the first measurement series has to cover the flow without control. The only parameter subject to variation is the total temperature drop ΔT between the bottom heater and the top heat exchanger. Even though the surface is cooled only partially, the system may be described by the Grashof number

$$\mathrm{Gr} = \frac{\beta \, \mathrm{g} \, \Delta T \, \mathrm{H}^3}{\nu^2} \qquad (2)$$

where β, g, and H are volumetric expansion coefficient, acceleration of the free fall, and height. For Rayleigh-Bénard systems with homogeneous upper and lower temperature boundary conditions, a flow phenomenon often termed wind is known. Instead of an axi-symmetric convective pattern, fluid rising in a more or less kidney-shaped region at one side, moving along the surface to the opposing side, descending there, and closing the loop along the bottom is frequently observed. It was not expected to find any wind in the system with partially cooled surface because of the primary strong horizontal temperature gradient at the perimeter of the heat exchanger directed radially everywhere, which gradient should lead to kind of a forced symmetrisation. Quite the contrary, the wind always showed up as the sole and stable flow pattern for all Gr - albeit in statistical orientation.

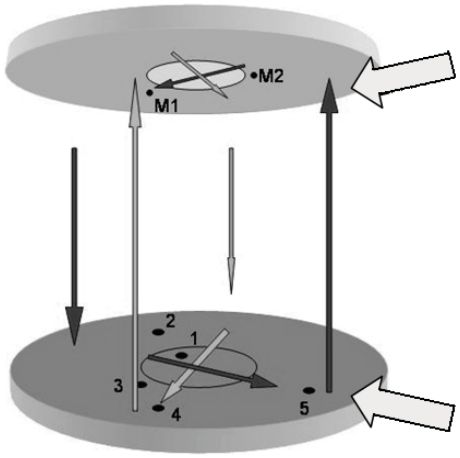

Figure 2: Statistically oriented flow directions. The big grey arrows indicate the UDV sensor positions.

This mono-cellular pattern was detected as an asymmetry in the temperature data recorded with both tripods, and confirmed by UDV measurements. Fig. 2 shows schematically both such statistically oriented flow directions and the position of the ultrasonic sensors, whereas Fig. 3 illustrates the measured ultrasonic velocity profiles for several temperature gradients and gives evidence to the previously described wind.

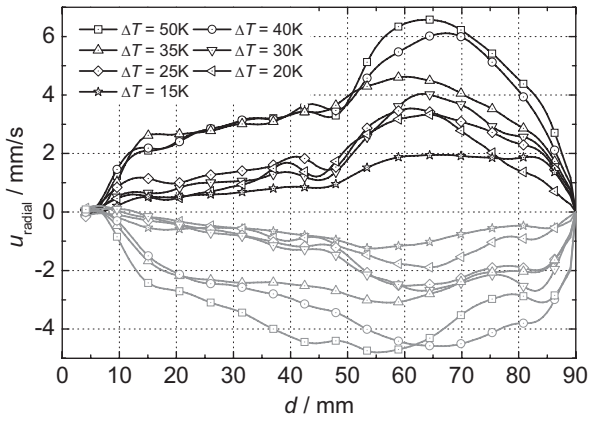

Figure 3: UDV profiles of the wind for several temperature gradients between heater and cooler. Positive values (upper sensor) indicate a flow away from the sensor, negative values (lower sensor) a flow toward the sensor.

When the RMF is switched on the wind starts to rotate as indicated schematically in Fig. 4. By analogue with the superposition of the primary and the secondary flow in an RMF, the swirl evoked by the RMF is also superimposed to the wind without any remarkable interaction. Not until the weaker secondary flow produced by the RMF becomes similar in vigour to the buoyant wind does the flow structure in the modified Rayleigh-Bénard system change basically. The scenario for strengths of the RMF below this threshold is shown in Fig. 5 in the form of a spatio-temporal representation of velocity.

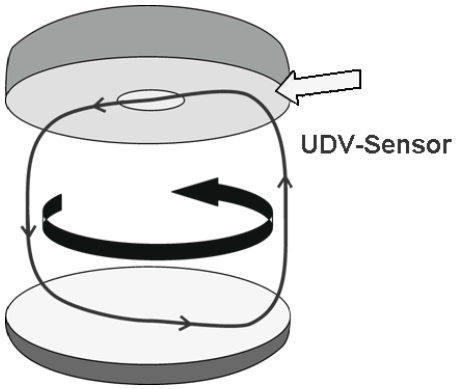

Figure 4: Schema of the buoyant wind co-rotating with the applied RMF.

Concerning the objective function without applying the RMF it arises $r^* \approx 3$. It is reminded that it should not be expected to observe highly precise and reproducible values for that magnitude. r^* is calculated from two differences out of three absolute measurements of temperature, each of the differences being quite small because of the short distance between the thermocouples. However, Fig. 6 evinces that r^* deteriorates for weak magnetic fields up to the threshold described above in the previous paragraph.

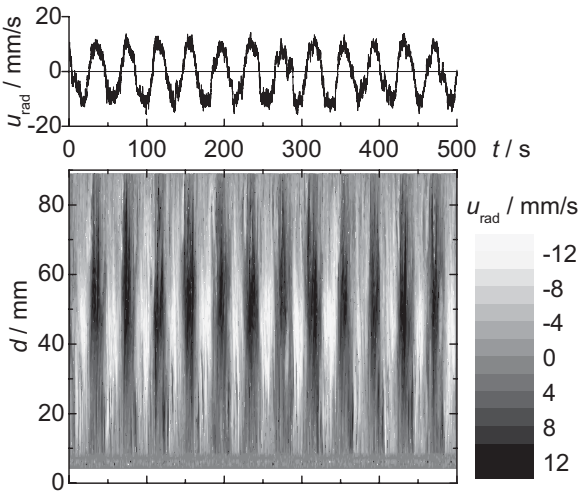

Figure 5: Dependence of the radial velocity component on time at Ta = $5 \cdot 10^5$ in a contour plot along the ultrasound beam (lower panel) and for a selected location (upper panel). While the RMF is weak the buoyant wind co-rotates with the magnetic field.

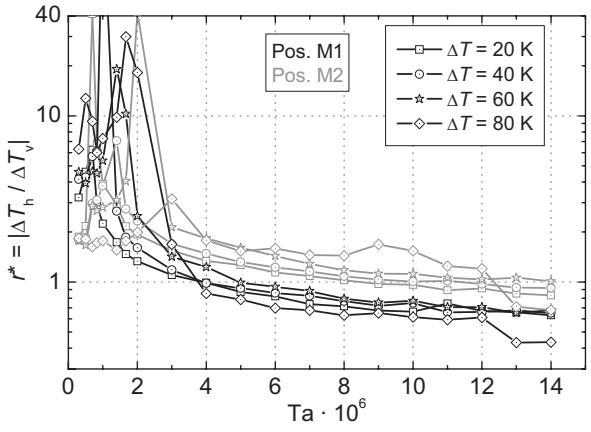

Figure 6: Dependence of the objective function r^* on the strength of the RMF.

Although the representation of the ordinate is logarithmic, the plot is cropped at the upper end – r^* reached values exceeding 100. Increasing the field strength leads to the secondary flow produced by the RMF forcing dominating the wind; r^* starts to decrease. As the mono-cellular buoyant flow structure vanishes completely above a certain value of Ta, Fig. 6 clearly shows that $r^* \approx 1$ is accomplishable whatever the vertically applied temperature difference. MULTIMAG would allow raising Ta for more than two orders of magnitude while the four ΔT contained in Fig. 6 are yet in the range of industrial interest ($Gr_{\Delta T=20K} = 1.7 \cdot 10^8$ … $Gr_{\Delta T=80K} = 1.1 \cdot 10^9$).

It is well known that an RMF may reduce the temperature fluctuations, which are inherent to turbulent natural convection. Hence, it was worth while to study also the transients of temperature. Fig. 7 shows the temperature signals recorded with one of the six thermocouples comprising the two tripods. The amplitude of the fluctuations decreases to 7% when Ta is increased about 50 times.

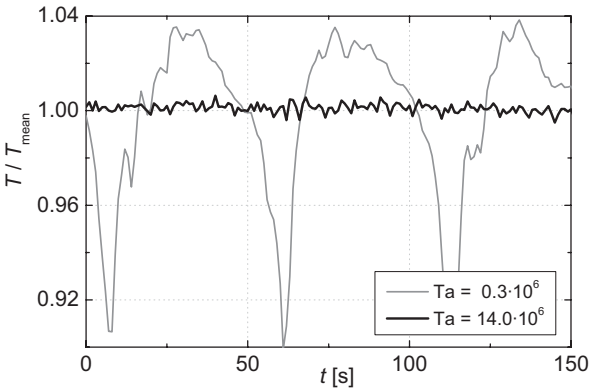

Figure 7: Temperature signals recorded at two different strengths of the magnetic field.

4 SUMMARY

Firstly, local gradients and fluctuations of the temperature field in the vicinity of the solid-liquid interface in a physical model of the Czochralski crystal growth process were studied experimentally. A comparable magnitude of the horizontal ΔT_h and the vertical temperature gradient ΔT_v at the triple point melt-crystal-atmosphere was chosen as a target function for an optimisation via electromagnetic flow control. It is shown that this task may be accomplished yet with an RMF alone: for any vigour of the buoyant convection investigated in the experiments. The application of RMF also reduced the temperature fluctuations.

Secondly, for flow measurements, the UDV technique was proved as a valuable tool in the detection and the characterisation of non-axisymmetric convective patterns.

5 ACKNOWLEDGEMENTS

This work was financially supported by “Deutsche Forschungsgemeinschaft” in the framework of the Collaborative Research Centre SFB 609.

REFERENCES

[1] Gorbatchev L P et al: Magnetohydrodynamic rotation of an electrically conductive liquid in a cylindrical vessel of finite dimensions, Magnetohydrodynamics 10 (1974) 406-414.

[2] Davidson P A, Hunt J C R: Swirling recirculating flow an a liquid-metal column generated by a rotating magnetic field, J. Fluid Mech. 185 (1987) 67-106

[3] Takeda Y: Development of an ultrasound velocity profile monitor, Nucl. Eng. Design 126 (1991) 277-284.

[4] Cramer A et al.: Local flow structures in liquid metals measured by ultrasonic Doppler velocimetry, Flow Meas. and Instrum. 15 (2004) 145-153.

[5] Pal J et al.: MULTIMAG – A MULTIpurpose MAGnetic system for physical modelling in magnetohydrodynamics, Flow Meas. Instr. 20 (2009) 241-251.